International Core Journal of Engineering Volume 6 Issue 4, 2020
ISSN: 2414-1895 DOI: 10.6919/ICJE.202004_6(4).0004

Mechanism Design and Simulation Analysis of a New Baggage Diversion Lifting Mechanism

Lin Huang *， GuoLin Li.

Sichuan Aerospace Tuoxin basalt Industry Co., Ltd, Chengdu, China.

*Corresponding author e-mail: 839263798@qq.com.

Abstract

A new type of baggage diversion lifting mechanism is proposed, which is driven by an electronic cylinder and a parallelogram mechanism to realize lifting and reset function. It can meet the requirements of small working space and lifting stroke, and has a simple structure. The parameter design of the mechanism is completed, and the dynamics and kinematics analysis of the mechanism are carried out. The driving force and the joint forces are obtained to verify the feasibility of the lifting mechanism, which provides the basis for the selection of the driving element and the optimization of the mechanism design.

Keywords

Baggage diversion; Lifting mechanism; Dynamics and kinematics analysis.

1. Introduction

With the rapid development of the aviation industry, the passenger and cargo throughput of civil aviation airports has grown at a rapid rate. The traditional baggage diversion equipment has been unable to meet the need for rapid growth of airport baggage traffic [1]. For this reason, it is of great significance to study a device for realizing rapid baggage diversion. Lifting mechanisms are widely used in logistics, handling, loading and unloading, etc., and are also the core part of baggage diverting devices.

At present, common lifting mechanisms include rack and pinion lifting mechanism, screw-type lifting mechanism, and scissor lifting mechanism[2]. Many scholars have studied the structural performance[3] and optimized design[4] of the rack and pinion mechanism, which has the features of continuous work, fast lifting speed and good synchronization. The screw-type lifting mechanism has the features of simple structure, convenient manufacture and reliable operation, and the research is also relatively extensive, mainly on the aspects of parameter design[5] and transmission theory[6]. The scissor lifting mechanism has the features of compact structure and large bearing capacity, and the main research contents are fatigue life[7] and mechanism optimization design[8].

Although these studies have promoted the wide application of lifting mechanisms, the existing lifting mechanisms are mainly applicable to occasions where the work space and work stroke are large, thus cannot meet the work requirements of baggage diversion. This paper proposes a new type of baggage diversion lifting mechanism, which is driven by an electronic cylinder and a parallelogram mechanism to realize the lifting and reset function. It can meet the working requirements of small working space and lifting stroke, and has a simple structure.

In addition, with the advent of dynamics and kinematics analysis software, many scholars have used software to study the design of the organization, which provides guidance for the optimal design of the organization and greatly shortens the time for design and development. And the simulation analysis can be realized by using ADAMS software. Ge et al. used ADAMS software to study the

ISSN: 2414-1895 DOI: 10.6919/ICJE.202004_6(4).0004

kinematics and dynamics[9-11] of the lifting mechanism. Zhang et al. used ADAMS software to optimize the design of the lifting mechanism [12].

This article will study from the analysis of baggage diversion, mechanism design and simulation analysis of the new lifting mechanism.

2. Baggage Diversion Process and Technical Requirements

2.1 Baggage Diversion Process

The baggage diversion process as shown in Figure 1. The baggage is placed on the tray, the tray is driven by the conveyor belt or the electric cone roller, and the essence of the baggage diversion is to change the direction of the tray. When the lifting mechanism is in the reset state, the lifting mechanism is lower than the surface of the conveyor belt. At this time, the tray and baggage moving in the direction of the speed V move along the V_1 direction under the action of the conveyor belt. When the lifting mechanism is in the lifting state, the lifting mechanism is slightly higher than the belt surface, so the tray and baggage leave the conveyor belt, and start to change direction under the drive of the electric cone roller. When the tray and baggage leave the lifting mechanism, it move in the V_2 direction to achieve baggage diversion.

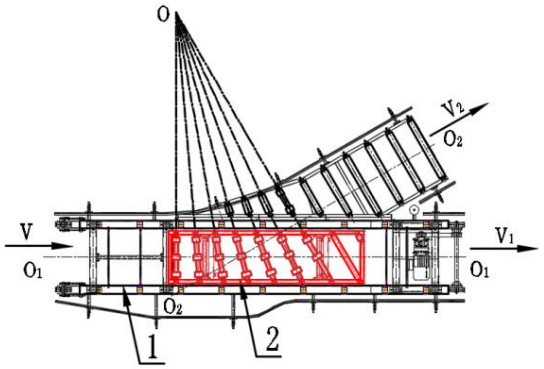

Figure 1. Baggage diversion process.1 Conveyor belt, 2 Lifting mechanism

2.2 Baggage Diversion Technical Requirements

The design requirements for the new package conveyor are as follows:

• The ability to divert baggage is 2.25s/piece;

• The velocity of the tray and baggage during the diversion process is 2500mm/s;

• The maximum number of baggage transported by the lifting mechanism is 1;

• The maximum mass of tray and baggage is 105kg;

• The maximum mass of support plate is 190kg;

• Plastic tray dimensions: 1350mm (length), 1000mm (width);

• Transport equipment reserved interface size: 2500mm (length), 700mm (width), 310mm (height);

• The total stroke of the lifting process or reset process is 24mm. When the lifting mechanism is in the reset state, the lifting mechanism is lower than the surface of the conveyor belt by 16mm. When the lifting mechanism is in the lifting state, the lifting mechanism is higher than the surface of the conveyor belt by 8mm.

3. The Mechanism Desing of New Lifting

3.1 Structure and Working Principle

A new type of baggage diversion lifting mechanism is proposed, and the kinematic sketch of mechanism as shown in Figure 2. The lifting mechanism consists of triangular arm ABC and EFG, electronic cylinder, Push rod BE, and support plate I_1-I_1. Points A and G are the revolute pairs of the triangular arm and the frame. Points B and E are the revolute pairs of the Push rod and the triangular

ISSN: 2414-1895 DOI: 10.6919/ICJE.202004_6(4).0004

arm. Points C and F are the revolute pairs of the support plate and the triangular arm. Point O is the revolute pair of the electronic cylinder and the frame. When the lifting mechanism is working, the electronic cylinder rod pushes the push rod to move first. Then the push rod pushes the triangular arm ABC and the triangular arm EFG to rotate around the revolute pairs A and G, respectively. Finally, the support plate completes the lift and reset functions under the action of the triangular arm. When the tray and baggage needs to be diverted, the lifting mechanism raises to the design position in advance. After the tray and baggage passes, the lifting mechanism is quickly reset.

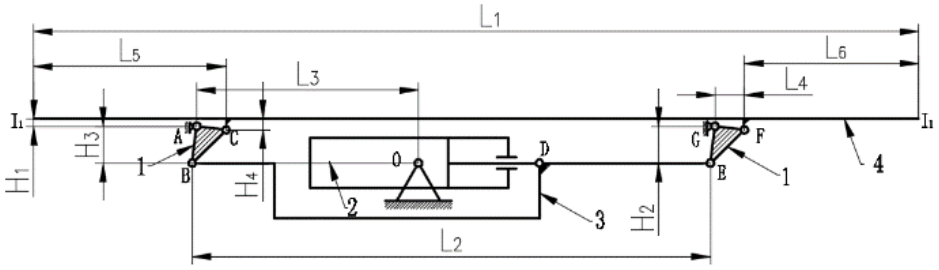

Figure 2. The kinematic sketch of mechanism.1 Triangular arm, 2 Electronic cylinder, 3 Push rod, 4 Support plate

3.2 Determination of Basic Dimensions

3.2.1 The length and width of the support plate

In order to ensure that the lifting and reset processes do not interfere with the conveyor equipment, the length and width of the support plate must be smaller than the reserved interface size. Therefore take the support plate length L_1=2390mm, width 640mm. In order to ensure that the stability of the baggage through the support plate, the distance from the revolute pair C to the left end of the supporting plate is taken as L_5 = 470mm, the distance from the revolute pair F to the right end of the supporting plate is taken as L_6 = 470mm. Due to the space limitation, the distance from the revolute pair C to the bottom surface of the support plate is taken as H_4 = 30 mm.

3.2.2 The position and basic size of the triangular arm

In order to ensure that the support plate does not interfere with the triangular arm when the lifting mechanism is in the reset state, the distance between the support plate and the revolute pair A must satisfy $H_1 \geq 20$mm, due to the space limitation, take H_1 = 21 mm. In order to ensure the structural symmetry of the lifting mechanism and the stability of baggage passing, the distance between the revolute pair A and G is taken as L_2=1400mm. In order to save energy, the ratio of input force and output force of lifting mechanism is 1:1.25. Therefore, the length of the triangular arm ABC is taken as L_{AB}=100mm, L_{AC}=80mm, L_{BC}=128mm; the length of the triangular arm GEF is taken as L_{GE}=100mm, L_{GF}=80mm, L_{EF}=128mm. At this time, the arm of force that the revolute pair B(E) to the revolute pair A(G) is H_2=99.2mm, the arm of force that the revolute pair C(F) to the revolute pair A(G) is L_4=79.4mm.

3.2.3 The length of the push rod

Due to the revolute pairs B and E is the hinge points of the push rod and the triangle arms, the length of the push rod is equal to the distance between the revolute pairs B and E, which is also equal to the distance between the revolute pairs A and G. So the length of the push rod is 1400 mm.

3.2.4 The position of the electronic cylinder

Due to the space limitation, the horizontal distance between the rotating pair O and the rotating pair A is taken as L_3=600mm, the vertical distance is taken as H_2=99.2mm. Therefore, the distance H_4 which between the revolute pair O and the ground is

$$H_4 = 310mm - H_1 - H_2 = 189.8mm. \quad (1)$$

ISSN: 2414-1895 DOI: 10.6919/ICJE.202004_6(4).0004

3.3 Electronic cylinder output force calculation

When the baggage passes through, the lifting mechanism always maintains the instantaneous static balance due to the action of the electronic cylinder. From the section 3.2, we get

$$F_2 : F_1 = H_2 : L_4 = 1 : 1.25 \tag{2}$$

where F_1 is the force of the support plate to the triangular arm, F_2 is force of the push rod to the triangular arm.

From the section 2.2, the mass of the tray and baggage is 105kg, the mass of the support plate is 190kg. Gravity acceleration is taken as 10m/s^2. According to the law of Newton's movement, the force F_1 is equal to the sum of the gravity of the support plate, tray and baggage. We get

$$F_1 = (m_1 + m_2) \times G = 2950N \tag{3}$$

where m_1 is the mass of the tray and baggage, m_2 is the mass of the support plate, G is the gravity acceleration.

So the force F_2 is

$$F_2 = F_1 / 1.25 = 2360N. \tag{4}$$

Because the rotation angle of the electronic cylinder is very small (less than 0.5°) at this time, the output force of the electronic cylinder is approximately equal to the force F_2. We get

$$F \approx F_2 = 2360N \tag{5}$$

where F is the force of the electronic cylinder.

3.4 Determination the total time of the lifting and reset stroke

During the diversion process, the time for the tray and baggage to pass through the lifting mechanism is t_1, the stroke is S, and the speed is V. From the section 2.2, we take S=3850mm, V=2500mm/s. According to the law of Newton's movement, we get

$$t_1 = S / V = 3850 / 2500s = 1.54s. \tag{6}$$

So the total time of the lifting and reset stroke should meet

$$t \le t_2 - t_1 = 0.71s \tag{7}$$

where t is the total time of the lifting and reset stroke, t_2 is the time to divert a piece of baggage, and from the section 2.2, we can get t_2=2.25s.

3.5 Determination of input motion during lifting and reset

In order to meet the lifting and reset time requirements of the lifting mechanism, the input motion of the mechanism needs to be designed. The cylinder rod drives the push rod directly, so the input motion can be expressed by the movement of the cylinder rod. In order to make the mechanism run smoothly both in the process of lifting and reset, the cylinder rod does a uniform acceleration first, then a uniform motion, and finally a uniform deceleration. From the section 3.4, we can get the maximum total time of the lifting and reset stroke is 0.71s, here take t=0.6s, and the lifting process and reset process time are both 0.3s.

From the section 2.2, it is known that the total stroke of the lifting process or reset process is 24mm. From the section 3.2, it is known that the ratio of input force and output force of lifting mechanism is 1:1.25. So we can take the stroke of the cylinder rod is 30mm.

During the lifting process, the time for each part of the lifting process is the same. We get

$$V_{P1} \times 2t_3 = S_1 \tag{8}$$

ISSN: 2414-1895 DOI: 10.6919/ICJE.202004_6(4).0004

where V_{P1} is the peak speed of the cylinder rod, t_3 is the time for each part of the lifting process, and t_3=0.1s, S1 is the stroke of the cylinder rod. It can be got that V_{P1}=150mm/s by the above equations. So get the relationship between cylinder rod speed and time in lifting process as shown in Figure 3.

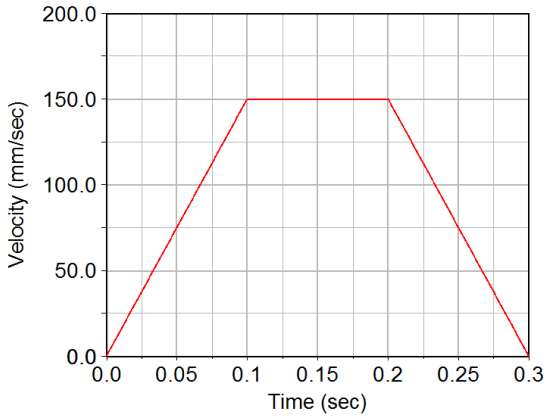

Figure 3. Relationship between cylinder rod speed and time in lifting (reset) process

During the reset process, the time for each part of the lifting process is the same. We get

$$V_{P2} \times 2t_4 = S_1 \tag{9}$$

where V_{P2} is the peak speed of the cylinder rod, t_4 is the time for each part of the reset process, and t_4=0.1s, S_1 is the stroke of the cylinder rod. It can be got that V_{P2}=150mm/s by the above equations. So get the relationship between cylinder rod speed and time in reset process as shown in Figure 3.

4. Kinematics and Dynamics Simulation Analysis of New Lifting Mechanism

According to the design of the new lifting mechanism, 3D model of the lifting mechanism is built and the multi-body kinematics and dynamics simulation analysis is carried out. Because the lifting mechanism is at rest when baggage passes through, and the cylinder output force during this process has been determined in the previous calculation, only lift and reset processes of the lifting mechanism is simulated in this paper.

4.1 Kinematics and Dynamics Modeling of New Lifting Mechanism

4.1.1 Geometry Model of New Lifting Mechanism

The model of the lifting mechanism was built with PROE software, which is shown in Figure 4, and is imported into ADAMS software after simplifying it, as shown in Figure 5.

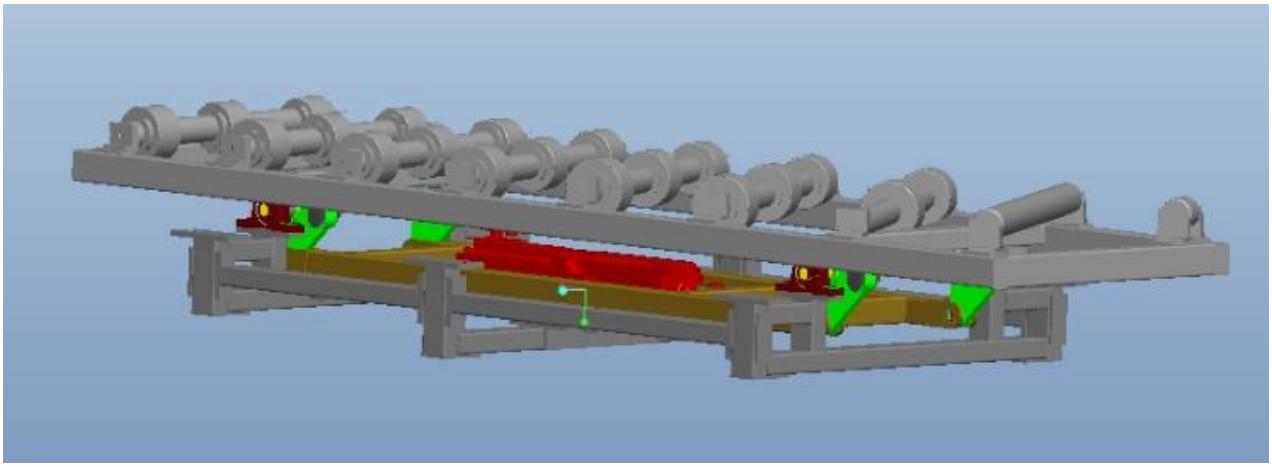

Figure 4. 3D model of the lifting mechanism

ISSN: 2414-1895 DOI: 10.6919/ICJE.202004_6(4).0004

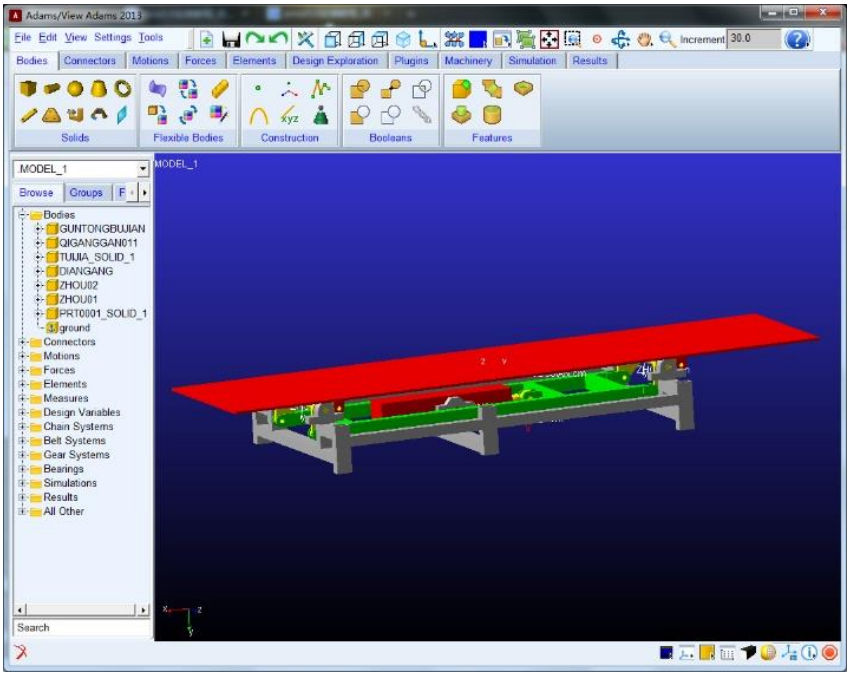

Figure 5. The interface of adams software after importing the model

4.1.2 Treatment of Constraints and Loads

In ADAMS, a system consists of multiple component elements. In order to simulate the actual movement of the system, the constraints within each component and drive constraint are needed to be defined. In the lifting mechanism model, the support plate and the triangular arm, the triangular arm and the push frame, the shaft and the bearing seat, the cylinder push rod and the push frame, and the electronic cylinder and the frame are respectively connected by revolute pairs; Cylinder push rod and cylinder are connected by moving pair; The triangular arm is fixed on the shaft; The bearing seat is fixed on the frame; The frame is fixed on the ground. Finally a linear drive is added to the cylinder push rod.

Because there is no baggage passing through the support plate during the lift and reset process, only the gravity of each component is considered in the simulation. In this paper, the support plate is given the mass of 190Kg, and the rest of the components are given as steel for simulation analysis. Because the friction between each pair of motions is ignored, the force obtained by the simulation will be less than the actual force. In the actual calculation, a certain safety factor should be taken.

4.2 Analysis Results and Discussion

According to the relationship between cylinder rod speed and time in Figure 3, kinematics and dynamics simulation is performed by using the step function in ADAMS software. And the simulation results are as follows:

4.2.1 Analysis of electronic cylinder output force

Throughout the lifting and reset process, the electronic cylinder output force changes over time as shown in Figure 6. The first 0.3s is the lifting process , and the remaining 0.3s is the reset process. During the lifting process, the direction of the electronic cylinder output force is consistent with the direction of movement, the electronic cylinder does positive work. During the reset process, the direction of the electronic cylinder output force is opposite to the direction of movement, the electronic cylinder does negative work. The maximum output force of the electronic cylinder push rod during the entire process is 1710.80N.

ISSN: 2414-1895 DOI: 10.6919/ICJE.202004_6(4).0004

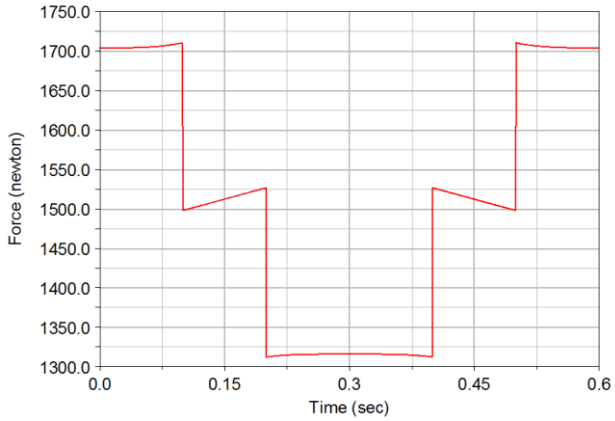

Figure 6. Output force of electronic cylinder changing over time

4.2.2 Analysis of the lift height

In order to verify that the lift height meets the technical requirements, the lifting height of the support plate needs to be analyzed. And the lifting height of the support plate changes over time as shown in Figure 7 According to the figure, the lifting height of the support plate is 166.66-142.65mm=24.01mm, which meets the design requirements.

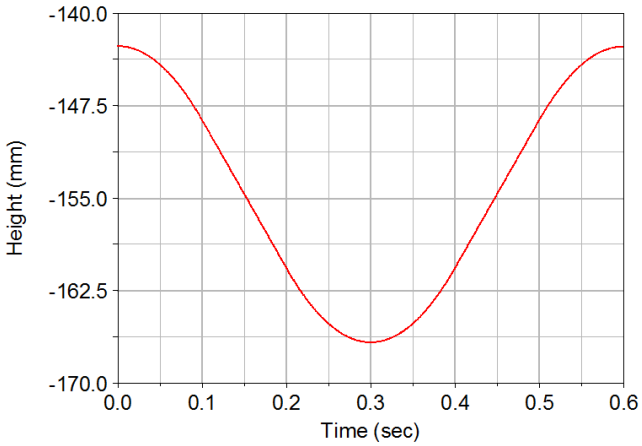

Figure 7. Lifting height of the support plate changing over time

4.2.3 Analysis of joint force

Throughout the lifting and reset process, the forces in the X-axis direction and the Y-axis direction at each joint change over time as shown in Figure 8 and Figure9. The maximum force of the revolute pair A in the X-axis and Y-axis directions is 834.41N and 1137.31N respectively, and the peak value of the resultant force is 1410.57N. The maximum force of the revolute pair B in the X-axis and Y-axis directions is 812.82N and 70.71N respectively, and the peak value of the resultant force is 815.76N. The maximum force of the revolute pair C in the X-axis and Y-axis directions is 41.12N and 1011.07N respectively, and the peak value of the resultant force is 1011.46N. The maximum force of the revolute pair D in the X-axis and Y-axis directions is 1710.54N and 37.99N respectively, and the peak value of the resultant force is 1710.80N. The maximum force of the revolute pair E in the X-axis and Y-axis directions is 872.39N and 71.85N respectively, and the peak value of the resultant force is 875.16N. The maximum force of the revolute pair F in the X-axis and Y-axis directions is 0.0N and 1082.33N respectively, and the peak value of the resultant force is 1082.33N. The maximum force of the revolute pair G in the X-axis and Y-axis directions is 870.84N and 1211.19N respectively, and the peak value of the resultant force is 1491.76N. The maximum force of the revolute pair O in the X-axis and Y-axis directions is 1719.46N and 349.70N respectively, and the peak value of the resultant force is 1752.72N. These data show changes in the force on the

ISSN: 2414-1895 DOI: 10.6919/ICJE.202004_6(4).0004

kinematic pairs during the movement of the lifting mechanism, which further provide data basis for checking the strength of the mechanism and the selection of bearings.

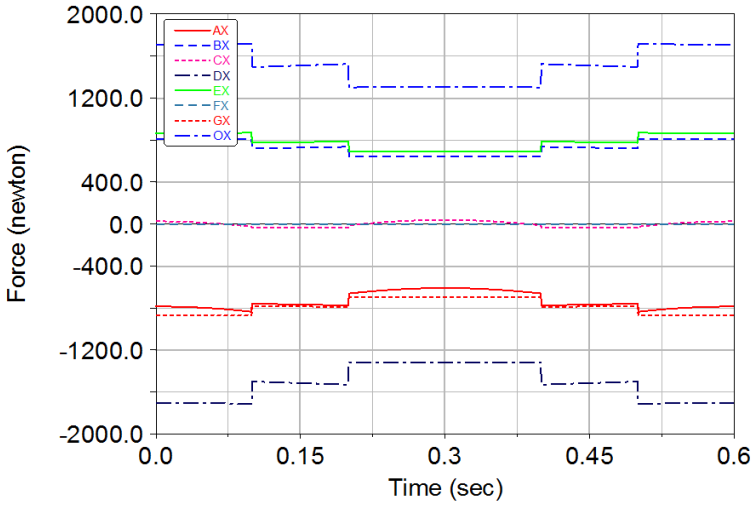

Figure 7. Forces of X-axis direction at each joint changing over time

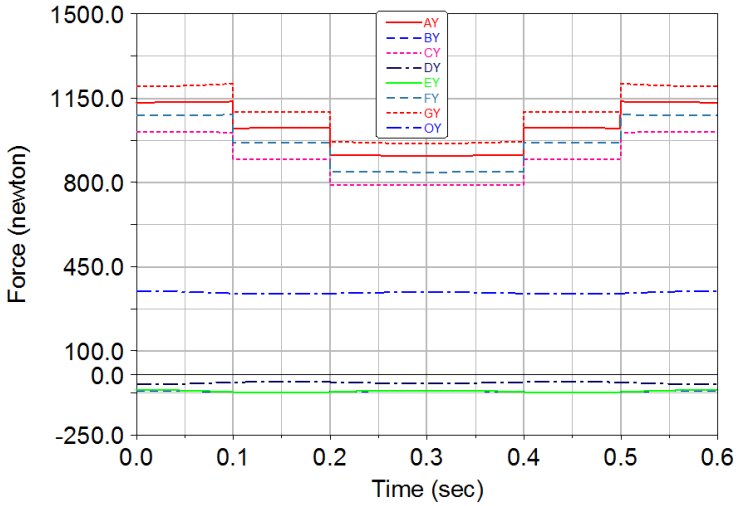

Figure 8. Forces of Y-axis direction at each joint changing over time

5. Conclusion

This paper proposes a new baggage diversion lifting mechanism whose working principle is simple, structure is compact and lifting stroke is small. Following conclusions can be drawn from the study:

The lifting mechanism is mainly consists of a electronic cylinder and a parallelogram mechanism. And the basic dimensions have been determined.

The output force of the electronic cylinder is 2360N when baggage passes.

Kinematics and dynamics analysis of the lifting and reset strokes on the new baggage diversion lifting mechanism is completed. The direction of the output force of the electronic cylinder is unchanged during the whole process and the maximum value is 1710.80N. During the lifting process, the electronic cylinder does positive work. During the reset process, the electronic cylinder does negative work. In this paper, we also get the loading data of all joints, and get that the maximum force on each kinematic pair appears, which provide a reliable basis for the selection of power element and standard parts and the optimization of mechanism design.

ISSN: 2414-1895 DOI: 10.6919/ICJE.202004_6(4).0004

References

[1] A. Abdelghany, K. Abdelghany, and R. Narasimhan, "Scheduling baggage-handling facilities in congested airports," Journal of Air Transport Management, 2006, vol. 12(2), pp. 76-81.

[2] G. Du, "Analysis of research status of lifting mechanism of lifting platform," Mechanical Engineering and Automation, 2013(02), pp. 205-207.

[3] G. Wang, X. W. Meng, and M. Peng, "Structural design and analysis of self-elevating platform support lift system," Mechanical Design, 2011(07), pp. 42-46.

[4] C. H. Xu, T. Lu, and G. M Chen, "The optimum dynamic analysis of misalignment of self-elevating platform rack and pinion lifting mechanism," Journal of Mechanical Engineering, 2014(19), pp. 66-72.

[5] Z. H. Zhai, Z. H. Ge, and K. K. Zhang, "Design and analysis of parallel four-bar lifting mechanism driven by screw nut," Journal of Shaanxi University of Science and Technology (Natural Science Edition), 2012(01), pp. 36-39.

[6] F. Zhou, X. Xu, and H. Zhang, "Transmission theory analysis of a dynamic spiral combination lifting mechanism," Energy Procedia, 2016, vol. 100, pp. 526-531.

[7] Y. J. Jia, "Analysis of fatigue life of lifting mechanism of an airport lifting platform," Journal of Military Transportation College, 2016, pp. 48-52.

[8] T. Liu and J. Sun, "Simulative calculation and optimal design of scissor lifting mechanism," Chinese Control and Decision Conference, 2009, pp. 2133-2136.

[9] X. K. Ge, D. W. Liu, and L. L. Zhu, "Fatigue life analysis of lifting mechanism rod based on virtual prototyping and FEM," Advanced Materials Research, 2013, vol. 680, pp. 364-368.

[10] W. H. Xu, C. S. Zhang, and S. Y. Wang, "Design and simulating analysis of compressed garbage transport truck lifting mechanism based on ADAMS," Applied Mechanics & Materials, 2012, vol. 215-216, pp. 1224-1227.

[11] M. Y. Zhao, H. L. Yan, and J. Wang, "Design and simulation of dump truck lifting mechanism based on ADAMS," Mechanical Engineering and Automation, 2012(02), pp. 64-66.

[12] G. J. Zhang, W. L. Ma, and J. J. Zhang, "Optimization of the position of the articulation joint of the hydraulic lifting cylinder of dump truck based on ADAMS," Machine Tool and Hydraulics, 2017(04), pp. 115-121.